

# A Novel Smart Driver Assistance System to Reduce Traffic Congestion Using Metaheuristic Algorithms and Deep Learning Methods

Omar Abdullah Hasan<sup>1\*</sup>, Duraid Y. Mohammed<sup>2</sup>

<sup>1,2</sup>Department of Computer, College of Engineering, Al-Iraqia University, 00964, Iraq  
Email: Omar.a.Hasan@aliraqia.edu.iq<sup>1</sup>, duraidyehya19@gmail.com<sup>2</sup>

\*Corresponding Author

---

Received: 15.03.2024

Revised: 10.04.2024

Accepted: 14.05.2024

---

## ABSTRACT

Cities across the globe have faced serious challenges of road accidents and traffic jams in recent days thereby increasing huge human and economic losses. The key to improving Advanced Driver Assistance Systems (ADAS) is precise analysis and modeling of driver behavior in complex driving scenarios. To deal with such challenges, acoustic-based ADAS systems have come into the limelight due to their cost-effectiveness and versatility. In this study, we suggest an AI-based Intelligent transportation system with smart ADAS technology to improve road safety and reduce traffic jams using acoustic data analysis techniques. We enhanced our integrated ITS and ADAS system using three acoustic datasets: IDMT Traffic for traffic assessment, LSA Vehicles for emergency sirens and road noise analysis, and RQA Road for road quality evaluation. The proposed methodology includes signal preprocessing by eliminating undesirable artifacts from the sound data, performed with a modified coati optimization (MCO) algorithm. Afterward, a feature extraction phase employs the Y-Net pretrained architecture that reveals hidden features that were optimized by the Emperor Penguin Optimization (EPO) algorithm to address dimensionality issues. Finally, a Recurrent Artificial Neural Network (RANN) with hybrid recurrent features is used to detect abnormalities in roadways and provide recommendations for drivers. The validation results on three benchmark datasets show promising results for prediction accuracy and false positive rate. The global results conclude that the proposed solution realized a superior classification accuracy score (96.252 %), precision (0.95), recall (0.94), and F-scores (0.95) compared to various baseline methods such as SVM, XG-Boost, t-SNE, CNN+LSTM, and SVM+LSTM.

**Keywords:** Advanced driver assistance systems, modified coati optimization (MCO), Y-Net pre-trained architecture, Emperor Penguin Optimization (EPO), Recurrent Artificial Neural Network

## 1. INTRODUCTION

The fast-growing nature of urbanization and the increasing number of vehicles on city roads everywhere in the globe is leading to some serious challenges such as accidents and traffic congestion[1]. These cases not only claim human lives on a large scale but also cause economic loss that in turn causes cities to lag. Human involvement is one of the main reasons for these problems, which can be related to low concentration, distractions, lack of experience, tiredness, and drowsiness. To overcome these issues and boost the effectiveness of today's Advanced Driver Assistance Systems (ADAS), we have to get exact insights and modeling of the driver behavior which could be later on implemented by the system. Specifically, these systems leverage deep learning (DL) to boost driver safety by analyzing complex real-time data from sensors and cameras. DL models enable features like object detection for collision avoidance, lane-keeping, and adaptive cruise control, improving the system's ability to navigate dynamic environments[2]. These AI-driven advancements are crucial for developing semi-autonomous and autonomous vehicles.

Actuators and sensors are the foundation of the majority of advanced aid technologies used in ADAS systems. These components play a crucial part in the development of the automotive industry[3], as demonstrated by the vision sensors that identify traffic signs. Such systems aim to process the intricate aspects of vision, making it possible for computers to recognize and process images or videos like humans do[4]. AI, more specifically Deep Learning (DL) has demonstrated this duality by making significant strides and surpassing humans in several tasks involving object identification and recognition[5]. To furnish drivers with a smart, secure, and agreeable driving experience, present-day vehicles coordinate

ADAS by utilizing a combination of active and passive sensors, including technologies like lidar and radar[6]. DL algorithms process the vast amounts of data from these sensors to detect objects, predict driver behavior, and make real-time decisions. Additionally, advanced signal processing techniques enhance the accuracy of sensor inputs by filtering noise and improving the detection of critical features, thereby boosting the overall performance of ADAS.

Recently, Metaheuristic-based CNN optimization methods such as genetic algorithms, particle swarm optimization, simulated annealing, and ant colony optimization, have shown a significant role in AI-based multi-modal intelligent systems by boosting the effectiveness and efficiency of CNN models[7]. In contrast to conventional optimization techniques that require explicit representations of the problem structure or derivatives, metaheuristic algorithms are driven by high-level strategies that are related to natural phenomena, social behavior, or a mathematical principle[8]. Such algorithms work in the form of black boxes without assuming that the mathematical characteristics of the problem are known, increasing their broad applicability even to the types of optimization problems that have complex and dynamic environments. In addition, Metaheuristics are powerful in suppressing noise levels in data through the optimization processes which will increase the data quality and reliability and finally make it more suitable for forthcoming analysis tasks. In the same manner, among the metaheuristic algorithms, dimensionality reduction happens to have the best shot at finding the subsets of features containing the primary information and discarding the trivial[9][10][11]. Techniques such as genetic algorithms and particle swarm optimization are designed to either navigate or search the most high-dimensional search spaces or find relevant feature subsets[12]. These techniques simplify data representations and save computational efficiency. Mixed-integer programming, hill-climbing-based algorithms, and swarm optimization can help greatly improve the analysis of low-dimensional data from fields like signal processing, machine learning, and beyond, due to their flexibility and scalability[13].

In this study, we have introduced an advanced AI-driven multi Intelligent Transportation System (ITS) that incorporates smart ADAS technology by combining various functionalities of two metaheuristics: (1) Modified coati optimization (MCO) algorithm[14], and (2) Emperor Penguin Optimization (EPO)[15] algorithm with a newly proposed Y-shaped CNN architecture. The MCO algorithm has shown a significant role in noise reduction in various research domains of engineering. Similarly, EPO is a new but advanced search space optimization technique to determine the most relevant and significant feature during acoustic data analysis. Here, the proposed CNN architecture was used to extract deep hybrid features from the smoothed signals and then the extracted features were optimized using EPO algorithm. Finally, the optimized sound features were classified using a novel Recurrent Artificial Neural Network (RANN) model. The primary objective of the proposed approach is to enhance road safety and mitigate traffic congestion. Our approach involves the meticulous analysis of three distinct acoustic datasets, each serving a specific purpose in assessing traffic conditions, analyzing emergency vehicle sirens and road noises, and evaluating road quality.

1. To ensure the quality of the acoustic signals, we implemented a signal pre-processing phase utilizing a modified coati optimization (MCO) algorithm, effectively removing unwanted artifacts.
2. Following signal pre-processing, we employed the Y-Net pretrained architecture for feature extraction, revealing intricate details in the acoustic data.
3. The extracted features underwent optimization through the Emperor Penguin Optimization (EPO) algorithm, addressing data dimensionality issues and ensuring the retention of pertinent features for subsequent analysis.
4. The final component of our proposed system is a hybrid Y-shaped CNN architecture, designed to detect abnormalities in road conditions. This RANN employs a multi-class classification system to provide valuable suggestions to drivers, contributing to a more intelligent, safe, and enjoyable driving experience.

The following is the structure of the remaining work. **Section 2** reviews the audit of existing works associated with the ITS for ADAS. The issue depiction and the proposed procedure are discussed in **Section 3** with the appropriate numerical capabilities. The outcomes and similar examination of proposed and existing shrewd transportation frameworks for savvy driver help are covered in **Section 4**. Finally, the conclusion and future scope are given in **Section 5**.

## 2. RELATED WORK

### 2.1 Baseline Models For Intelligent Transportation Systems

Several experiments have been carried out to enhance the efficiency of Advanced Driver Assistance Systems (ADAS). The details of few prominent studies are given in **Table 1**. In the past, models being used in Intelligent Transportation Systems (ITS) were predominantly based on statistical and heuristic models. But the emergence of deep learning (DL) has provided these systems with the basis to analyze data and

make decisions more accurately and flexibly with respect to the transport systems. For example, **Kim et al. (2017) [16]** have offered a means of estimating the risk of a collision that uses the lane-based probabilistic motion prediction of cars in the area to quantify the risk of a collision for a variety of local path options. Last but not least, each set of the tangential acceleration and the final lateral offset of the local path choices is represented by a trajectory plane. used to illustrate the collision risks. **Chen et al. (2017) [17]** have investigated road transport incidents involving hazardous materials that seriously endanger people's lives, property, and the environment. The purpose of this study is to examine hazardous material road transport accident data from seven regions of China using the eXtreme Gradient Boosting (XGBoost) algorithm. The suggested XGBoost approach offers the best modeling performance, according to the data.

**Nozaki et al. (2018) [18]** employ 5G wireless networks to transfer photographic images from trucks, cranes, and other construction equipment equipped with 4K cameras to a database. Artificial intelligence is then used to analyze worker interactions and movements inside the database. In this case, 4K photos from low-speed moving vehicles or cranes are sent to the database based on their speed and distance traveled to the 5G terminal that connects the base station and Internet of Things device. They analyze the relationship between the error of the system that uses AI to judge and identify the surrounding environment when video quality deteriorates, based on the error environment. **Zhang et al. (2018) [19]** presented an AI driven driver monitoring system to help drivers avoid accidents. The framework utilizes a two-layer long transient memory calculation to distinguish heart irregularities, a CNN architecture to recognize driver sluggishness from the scramble camera, and a front camera and GPS to recognize overspeeding. The proposed model integrates these inputs using a Neuro-Fuzzy controller, which then uses speed, heartbeat, and sleepiness variables to generate alerts and modulate brakes if needed.

**Singhal et al. (2020) [20]** have focused on the road vehicle-train collision risk prediction assessment enabled by AI, which could result in the creation of a road vehicle-train collision avoidance system for unmanned railway level crossings. The study's boundaries are set around single-line rail-road segments' unmanned level crossings where vehicles collide with trains on the road. The study's primary goal is to evaluate the risk of rail-road collisions by developing a model to forecast the frequency and severity of road vehicle-train collisions using Poisson and Gamma-log regression, respectively. **Saleem et al. (2022) [21]** have proposed the development of smart cities and transportation networks in the future is road traffic safety. The European Commission launched the emergency call initiative to assist drivers by setting up a special number. They looked into how to classify the severity of accidents involving powered two-wheelers using machine-learning techniques based on features that could be fairly acquired at the scene. It utilizes just eleven highlights to accomplish roughly 90% accuracy and review on a huge publically accessible corpus.

**Table 1.** Summary of research gaps in the existing studies

Ref.	Methodology	Technique used	Research gaps
Wen et al., (2021) [22]	Safety decision-making support	Multiple-input and output neural network	If the risk is high and might cause a collision
Das et al. (2022) [23]	Driving safety with sensing	Artificial intelligence-collision avoidance	It increases the average vehicle waiting time traveling efficiency and safety
Chang et al., (2017) [24]	Naturalistic driving study	T-distributed stochastic neighbor embedding (t-SNE)	High-quality sensors are expensive
Chen et al., (2016) [25]	Severity classification of accidents	Support vector machine (SVM)	It requires a lot of system resources which are not sufficient
Shen et al., (2020) [26]	Hazardous material road transport accident	XGBoost	A lot of overlapping information is involved in the inference process
Singhal et al. (2020) [20]	Road vehicle-train collision risk assessment	Poisson and Gamma-log regression	No load rate and energy consumption per mileage
Kim et al., (2017) [16]	Traffic collision risk assessment algorithm	Lane-based probabilistic motion	Not suitable for traffic regulation during rush hours
Tang et al., (2024) [27]	Road accident severity	CNN-LSTM	It does not support real-time conditions and causes traffic congestion
Feng et al., (2022) [28]	Prevent accidents in construction zones	Support vector machine (SVM) and LSTM	Complexity due to several sensors employed
Tonni et al. (2021) [29]	Driver vigilance system for accident prevention	Neuro-Fuzzy controller convolutional neural network	Inaccurate method need more data for training which limits the detection rate

### 3. PROPOSED METHODOLOGY

In this section, we explained the proposed AI-based multi ITS with smart ADAS for improving road safety by reducing traffic congestion using acoustic data analysis techniques.

#### 3.1 Overview of the Proposed Method

The overall system design of the proposed work, illustrated in **Figure 1**, involves a structured methodology comprising distinct phases. In the initial stage, data collection is carried out using various acoustic datasets, including the IDMT traffic dataset for assessing traffic conditions, the LSA vehicles dataset for analyzing emergency vehicle sirens and road noises, and the RQA road dataset for quality assessment of roads. Subsequently, the collected acoustic data undergoes a crucial signal pre-processing step aimed at eliminating unwanted artifacts, ensuring the accuracy of subsequent analyses. This involves the application of the modified coati optimization (MCO) algorithm to enhance the overall quality of the acoustic data. Following signal pre-processing, the pre-processed signal is subjected to feature extraction using the Y-Net pretrained architecture. This feature extraction phase aims to uncover hidden features within the acoustic data, providing a comprehensive understanding of underlying patterns. To address data dimensionality issues, the extracted features are then optimized using the emperor penguin optimization (EPO) algorithm, ensuring that the data remains informative and manageable. The subsequent abnormality detection phase involves the application of the hybrid CNN model to identify deviations from normal traffic patterns or road quality, leveraging the optimized features. Further, a multi-class classification is performed based on the nature of abnormalities detected in each dataset. For the IDMT traffic dataset, classes include Normal traffic and abnormal traffic. In the LSA dataset, classes comprise Vehicle sirens and Road noise. Lastly, the RQA dataset is divided into rough road, smooth road, and grassy road classes. Building on multi-class classification, the study defines smart driver assistance classes, including sudden acceleration (label-1), sudden right turn (label-2), sudden left turn (label-3), and sudden brake (label-4).

The proposed approach is briefly discussed in the subsequent subsections.

#### 3.1 Acoustic Data Pre-Processing

In this context, acoustic data pre-processing is a critical step aimed at enhancing the quality of the collected acoustic data by eliminating unwanted artifacts. The chosen method for this pre-processing task is the modified coati optimization (MCO) algorithm[14]. It operates as an optimization technique specifically designed for signal-processing applications. The MCO algorithm is employed to analyze and modify the acoustic data in a way that minimizes or eliminates undesirable elements, such as background noise, distortions, or irregularities, which may be present in the raw data. The algorithm utilizes an optimization process to adaptively adjust the parameters of a predefined model or filter, effectively suppressing unwanted components while preserving relevant information.

The modification process carried out by the MCO algorithm is tailored to the characteristics of acoustic signals, taking into account factors such as frequency, amplitude, and temporal patterns. Through iterative optimization, the algorithm refines its adjustments to achieve an optimal configuration that enhances the clarity and accuracy of the acoustic data. By applying the MCO algorithm for signal pre-processing, the unwanted artifacts within the acoustic data are effectively reduced or eliminated, resulting in a cleaner and more reliable dataset for subsequent analysis.

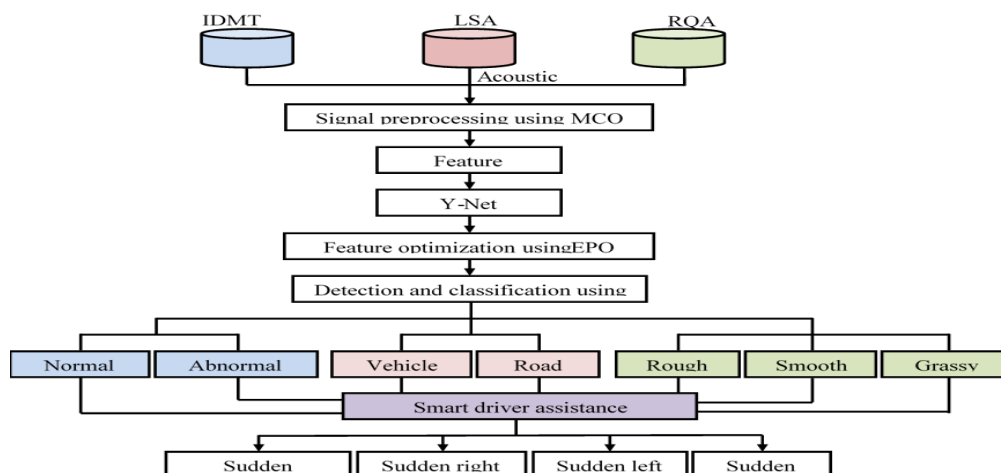


**Figure 1.** Overall system design of proposed work

The initialization of the MCO algorithm continues as before with the parameter initialization corresponding to the position of each coati. In the preliminary phase, the position of each coati is randomly defined by **Eq. 1**.

$$X_i : x_{i,j} = lb_j + r \cdot (ub_j - lb_j), i = 1, 2, \dots, N, j = 1, 2, \dots, m, \quad (1)$$

where  $X_i$  is the position of the  $i^{\text{th}}$  coati in search space,  $x_{i,j}$  is the value of the  $j^{\text{th}}$  decision variable,  $N$  is the number of coatis,  $m$  is the number of decision variables,  $r$  is a random real number in the interval  $[0, 1]$ , and  $lb_j$  and  $ub_j$  are the lower bound and upper bound of the  $j^{\text{th}}$  decision variable, respectively. The population of coatis in the COA is mathematically represented using the following matrix  $X$ , called the population matrix,

$$X = \begin{bmatrix} X_1 \\ \vdots \\ X_i \\ \vdots \\ X_N \end{bmatrix}_{N \times m} = \begin{bmatrix} x_{1,1} & x_{1,2} & \dots & x_{1,m} \\ \vdots & \vdots & \ddots & \vdots \\ x_{i,1} & x_{i,2} & \dots & x_{i,m} \\ \vdots & \vdots & \ddots & \vdots \\ x_{N,1} & x_{N,2} & \dots & x_{N,m} \end{bmatrix}_{N \times m} \quad (2)$$

The objective function ( $F_i$ ) of the problem is evaluated at various values as a result of the placement of potential solutions in variables. The fitness function matrix is given in the Equation (3).

$$\begin{bmatrix} F_1 \\ \vdots \\ F_i \\ \vdots \\ F_N \end{bmatrix}_{N \times m} = \begin{bmatrix} F(X_1) \\ \vdots \\ F(X_2) \\ \vdots \\ F(X_N) \end{bmatrix}_{N \times m} \quad (3)$$

where  $F_i$  is the objective function value derived from the  $i^{\text{th}}$  coati and  $F$  is the vector of the obtained objective function. The objective function's value refers to the quality of a candidate solution in COA. The process of updating the position of coatis (candidate solutions) in the COA is based on modeling two natural behaviors of coatis. These behaviors include (1) coatis' hunting strategy when attacking iguanas, and (2) coatis' escape strategy from predators. The study of the iguana attack's behavior correlates to the first stage of coati's population in the search space. One tactic involves having a group of coatis scale a tree to frighten the iguana away. A few more coatis are waiting for the iguana to fall to the ground from where they are caught beneath a tree. As the Iguana has fallen, to the floor, the coatis jump into it and catch it. Consequently, coatis shift their places in search space, and the COA exhibits its capacity to roam in global search inside its problem-solving domain. The position of the coatis is mathematically defined in Equation 4.

$$X_i^{p1} : X_{i,j}^{p1} = X_{i,j} + r \cdot (Iguana_j - I \cdot X_{i,j}), \text{ for } i = 1, 2, \dots, \frac{N}{2} \text{ and } j = 1, 2, \dots, m \quad (4)$$

In the search space, the iguana is positioned at random after it hits the ground. In the search space, which is simulated using Eqs. (5) and (6), coatis on the ground move based on this random position.

$$Iguana^G : Iguana_j^G = lb_j + r(ub_j - lb_j), j = 1, 2, \dots, m \quad (5)$$

$$X_i^{p1} : X_{i,j}^{p1} = \begin{cases} X_{i,j} + r \cdot (Iguana_j^G - I \cdot X_{i,j}) & F_{Iguana^G} < F_i \\ X_{i,j} + r \cdot (X_{i,j} - Iguana_j^G) & \text{else} \end{cases} \quad (6)$$

$$\text{for } i = \frac{N}{2} + 1, \frac{N}{2} + 2, \dots, N, \quad j = 1, 2, \dots, m$$

If each coati's new position enhances the value of the goal function, it is suitable for the update process; if not, the coati stays in its original location. This update condition is for  $i = 1, 2, \dots, N$  is updated according to Eq. 7.

$$X_i = \begin{cases} X_i^{p1}, & F_i^{p1} < F_i \\ X_i & \text{else} \end{cases} \quad (7)$$

Here,  $X_i^{p1}$  is the updated position calculated for the  $i^{\text{th}}$  coati,  $F_i^{p1}$  is its objective function value,  $r$  is a random real number in the interval  $[0, 1]$ .  $Iguana$  represents the iguana's position in the search space, which refers to the position of the best member,  $Iguana_j$  is its  $j^{\text{th}}$  dimension,  $I$  is an integer, which is randomly selected from the set  $1, 2$ .

The second step of the position of coatis update in the destitute region is modeled mathematically on the principle of foraging behavior of coatis when the coatis are encountered by predators and escape from the predators. A predator, in most cases, attacks coati from its sitting area. So, there is a tendency for an animal to exit that perch. This behavior of Coati can be interpreted as the COA that puts it in a position that is close to its current position, but it is safe; it is exploiting its near the search To emulate the mentioned situatedness, a partly random position is generated near the position of the coatis based on Eqs. (8) and (9).

$$lb_j^{local} = \frac{lb_j}{t}, \quad Ub_j^{local} = \frac{Ub_j}{t}, \quad \text{where } t = 1, 2 \dots T \quad (8)$$

$$X_i^{p2}: X_{i,j}^{p2} = X_{i,j} + (1 - 2r) \cdot (lb_j^{local} + r \cdot (Ub_j^{local} - lb_j^{local})), \quad \text{for } i = 1, 2, \dots, N \text{ and } j = 1, 2, \dots, m$$

$$X_i^{p1}: X_{i,j}^{p1} = \begin{cases} X_{i,j} + r \cdot (Iguana_j^G - I \cdot X_{i,j}) F_{Iguana^G < F_i} \\ X_{i,j} + r \cdot (X_{i,j} - Iguana_j^G) & \text{else} \end{cases} \quad (9)$$

The updated position is better if it enhances the value of the objective function, which this condition simulates using Eq. (10).

$$X_i = \begin{cases} X_i^{p2}, & F_i^{p2} < F_i \\ X_i & \text{else} \end{cases} \quad (10)$$

Here,  $X_i^{p2}$  is the updated position calculated for the  $i$ <sup>th</sup> coati,  $F_i^{p2}$  is its objective function value,  $r$  is a random real number in the interval  $[0, 1]$ .  $Iguana$  represents the iguana's position in the search space, which refers to the position of the best member,  $Iguana_j$  is its  $j$ <sup>th</sup> dimension,  $I$  is an integer, which is randomly selected from the set  $1, 2, \dots, t$  is the iteration counter,  $lb_j^{local}$  and  $Ub_j^{local}$  are the local lower bound and local upper bound of the  $j$ <sup>th</sup> decision variable respectively,  $lb_j$  and  $Ub_j$  are the lower bound and upper bound of the  $j$ <sup>th</sup> decision variable, respectively. The sample output for optimized signals (for 3 samples) is shown in **Figure 2**.

### 3.2 Feature Extraction And Optimization

Feature extraction and optimization are crucial stages in the proposed methodology, contributing to the comprehensive analysis of the pre-processed acoustic data. After the signal pre-processing phase, the enhanced data undergoes feature extraction to reveal hidden patterns. This process is facilitated by leveraging the Y-Net pretrained architecture, a neural network model designed for effective feature extraction from complex datasets. Y-Net pretrained architecture is employed to extract intricate features embedded within the acoustic data. This architecture, likely pre-trained on relevant tasks, possesses the capability to discern and highlight valuable information within the signals. The extraction of hidden features is used for obtaining a nuanced understanding of the underlying patterns present in the acoustic data. The process involved in the Y-Net for feature extraction can be described as follows:

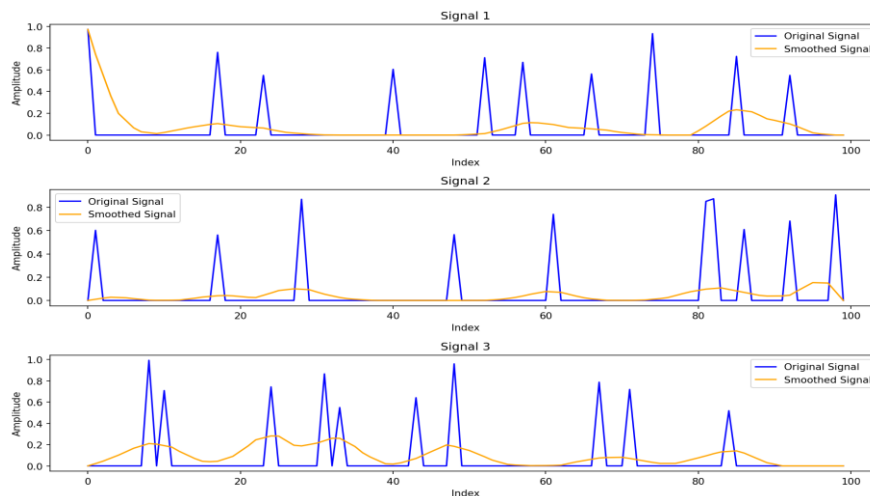


**Figure 2.** Signal smoothing (3 samples) using modified coati optimization

- The pre-processed acoustic data, refined through the signal pre-processing phase, serves as the input to the Y-Net for feature extraction.
- Y-Net refers to a neural network architecture that is pre-trained on relevant tasks, possibly in the domain of audio signal processing. It is used to effectively capture and represent intricate features present in complex acoustic datasets.
- The Y-Net comprises multiple layers, each responsible for extracting specific features from the input data. These layers may include convolutional layers, pooling layers, and fully connected layers, configured to discern hierarchical patterns within the acoustic signals.
- By leveraging knowledge gained from previous tasks for which the Y-Net was trained, the model can effectively generalize its feature extraction capabilities to the specific characteristics of the acoustic data under consideration.

- As the acoustic data passes through the layers of the Y-Net, it undergoes transformations that result in a hierarchically organized set of features. These features are representations of relevant patterns, structures, and information present in the acoustic signals.
- The extracted features are optimized to address data dimensionality issues. The emperor penguin optimization (EPO) algorithm is used for this, refining the representation of features to strike a balance between informativeness and manageability.
- The output of the Y-Net's feature extraction process is a set of optimized features that capture the essential characteristics of the pre-processed acoustic data. These features are then used as input for subsequent stages, such as abnormality detection and multi-class classification.

Following feature extraction, the obtained features undergo optimization to address potential data dimensionality issues. High-dimensional data can pose challenges in terms of computational efficiency and the risk of overfitting. To mitigate these challenges, the emperor penguin optimization (EPO) algorithm[15] is applied. The EPO algorithm serves as an optimization technique specifically tailored for dimensionality reduction, ensuring that the extracted features retain their informative content while reducing the overall data dimensionality. The optimization process performed by the EPO algorithm involves modifying the representation of features to increase their relevance and reduce redundancy. This leads to a more concise and manageable feature set that facilitates more efficient analysis and model execution. To show the discriminability among features, the variation in probability distribution before and after the feature reduction step is shown in **Figure 3**. Three other performance parameters (Mean, standard Variation, and Skewness) for original features and optimized features are also shown in **Figure 4**.

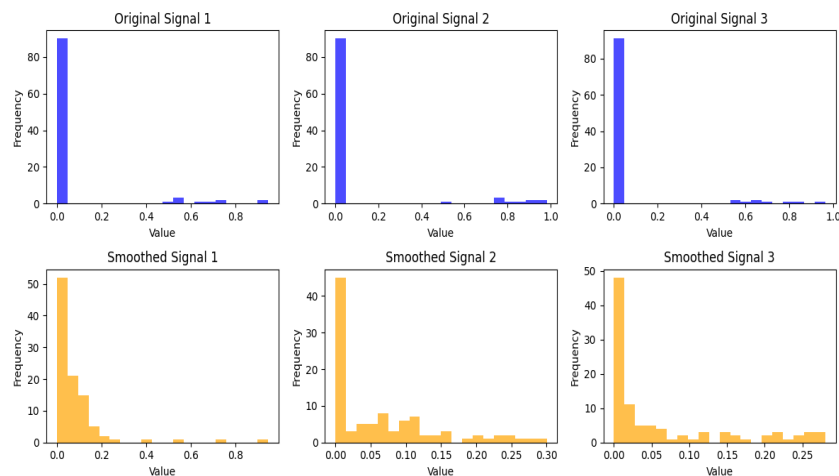


**Figure 3:** Variation in probability distribution function before and after the feature reduction step

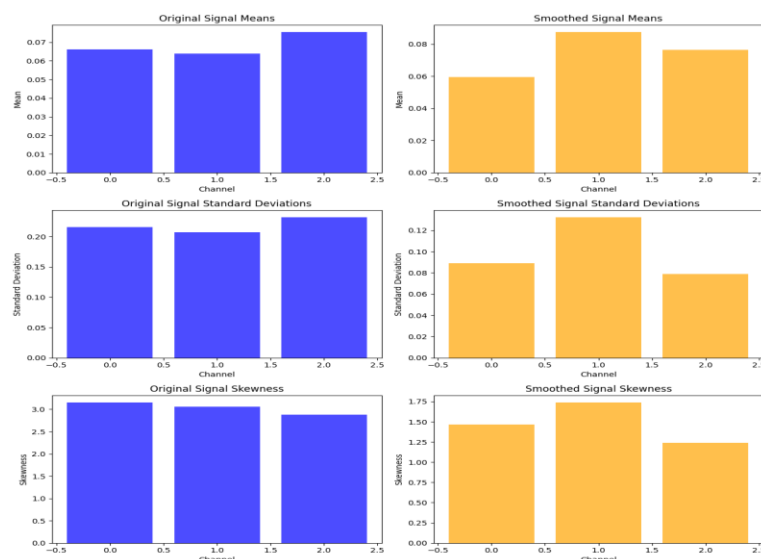


**Figure 4:** Variation in mean, standard variation, and skewness before and after the feature reduction step

### 3.3 Detection of road abnormality

The final stage of the proposed methodology involves the application of the hybrid recurrent artificial neural network (RANN) for the detection of abnormalities in road conditions, ultimately providing suggestions for drivers across various multi-class categories. The hybrid nature of the RANN implies a combination of recurrent neural network (RNN) elements, known for their sequential data processing capabilities, and artificial neural network components. The Hybrid RANN is trained to detect abnormalities in road conditions based on the patterns and features present in the input data. This includes identifying deviations from normal traffic patterns, recognizing emergency vehicle sirens or road noises, and pinpointing variations in road quality such as roughness, smoothness, or the presence of grass. The abnormalities detected lead to a multi-class classification system. For the RQA dataset, the classes comprise rough roads, smooth roads, and grassy roads, indicating variations in road quality. Building on the multi-class classification, the study further computes smart driver assistance classes, categorizing the detected abnormalities into specific driver assistance scenarios. These incorporate unexpected speed increase (mark 1), abrupt right turn (name 2), abrupt left turn (name 3), and unexpected brake (mark 4). Each class addresses what is going on that requires consideration or activity from the driver. Setting the suitable organization construction and finding the ideal boundary esteem incredibly influenced the ANN's presentation. The result can be determined from the accompanying condition:

$$S_p = f_p \left( \sum_{Q=1}^B W_{Q,p} M_Q + N_p \right) \quad (11)$$

where  $S_p$  donates the output of the node;  $Q_a$  is the  $Q$ -th input;  $W_{Q,p}$ , is the association boundary; addresses the inclination of the hub, and gives the hub move capability. In many occurrences, the hub move capability is nonlinear. As a repetitive model, the wellness capability is communicated as follows:

$$E(W(S)) = \frac{1}{B} \sum_{Q=1}^B \sum_{K=1}^K (o_{K,e} - o_{K,a})^2 \quad (12)$$

where  $E(W(S))$  and  $W(S)$  donate the mistake and boundaries in the conjunctions at the  $S$ -th emphasis, individually. The  $P$  addresses the quantity of examples and  $K$  addresses the quantity of result hub. The expected value of the  $K$ th output node is given by  $kE$ , and the actual value is given by  $ka$ ,  $O$ . ANN is a straightforward numerical model of the human cerebrum. The term can be found utilizing a RANN prepared to execute different conditions.

$$y^a x^b(y) = f(y, x(y), x'(y)), \quad (13)$$

Explicit BCs and  $a \in \mathbb{Z}$ ,  $\epsilon \in \mathbb{R}$ ,  $d \in \mathbb{R}$  address the space, and  $x(y)$  is the surmised arrangement. The problem takes on a particular shape if  $Q$ 's adjustable parameters serve as a test solution.

$$\text{Min}_j \sum_{Q_Q \in \mathbb{D}} f(y_Q, x_i(y_Q, j), x'_i(y_y, j)) \quad (14)$$

BC forced limitations. The experimental solver RANN is utilized in our proposed method, and the  $P$  parameters correspond to the neural structure's weights and biases. In many practical applications, ANNs are the most popular and widely used models because they are black-box tools. In the fields of hydro-environmental engineering, ANN modeling is frequently used for prediction. The articulation condition to decide the result worth of ANN is as follows.

$$\hat{x}_p = f_p \left[ \sum_{g=1}^M w_{PJ} \times f_g \left( \sum_{Q=1}^n w_{Yg} y_Q + Z_{ga} \right) + w_{Pa} \right] \quad (15)$$

where  $Q$ ,  $g$ ,  $P$ ,  $An$ , and  $w$  address the information, stowed away, and yield layers neurons, inclination and the applied weight (or predisposition) through the neuron, separately; mean actuation capability for the covered up and yield layers, individually;  $b$ ,  $a$  show individually input layer variable, number of information and number of stowed away neurons; what's more,  $x$ , represent noticed and processed upsides of the resulting neuron, separately. To get to memory we utilize an understanding regulator. The perusing regulator utilizes both the saw past direction and the unique situation  $(, )$  as key and produces a read likelihood over every memory area  $Q$ . A removal investigation of regulator variations is accounted for. We initially register a previous read similitude  $\pi$  and a setting read closeness as follows:

$$t_\pi^J = \frac{\pi^k \cdot \pi^Q}{\|\pi^k\| \|\pi^Q\|} \quad J = 0, \dots, |m| \quad (16)$$



$$t_\gamma^Q = \frac{\gamma^k \cdot \gamma^Q}{\|\gamma^k\| \|\gamma^Q\|} \quad Q = 0, \dots, |m| \quad (17)$$

We then feed  $t_\pi^J$  and  $t_\gamma^Q$  to a RANN F that mixes the read similarities, pondering past and setting position and can yield high scores for relevant examples and low scores for the others. The last perused probability is subsequently gotten as follows.

$$j(r)^Q = f(t_\pi^Q, t_\gamma^Q) \quad (18)$$

We simply read the top-K samples with the highest inference time to achieve multimodality because each memory sample can be read and decoded independently. This is accomplished by composing it as an amount of two terms. In our specific approach, the test solution  $x_i$  RANN is used, and the  $i$  parameters match the weight and dependence of the neural structure. For the test operation, we choose the form  $x_i(y)$  that satisfies the BCs. This can be achieved by writing a sum of two words:

$$x_i(Q_y, j) = n(y) + i(y, n(y, h)), \quad (19)$$

where is a solitary result RANN with injuries and B input units took care of with the information vector Q. The term includes no movable boundaries and items the BCs. The second term,  $g$ , is designed to satisfy the BCs without providing coverage. For a given info Y, the result of the RANN is figured as follows.

$$B = \sum_{Q=1}^g v_Q \sigma(z_Q), \quad \text{where } W_Q = \sum_{P=1}^B W_{QP} y_P + M_Q \quad (20)$$

where  $W_{QP}$  input unit Q epitomizes the heap that connects the secret unit to Q, the info unit Q describes the heap that joins Q to the result unit, and the secret unit portrays the reliance of Q, and is a sigmoidal transmission capability. The slant of the RANN is effectively gotten with esteem to the RANN settings.

$$\frac{\partial B}{\partial v_Q} = \sigma(W_Q), \quad (21)$$

$$\frac{\partial B}{\partial M_j} = v_Q \sigma'(W_Q), \quad (22)$$

$$\frac{\partial B}{\partial \omega_{QP}} = v_Q \sigma'(W_Q) y_P, \quad (23)$$

Hybrid RANN acts as the intelligent decision-making component of the system, detecting anomalies and providing information to drivers through multi-class classification. The resulting smart driver assistance classes provide drivers with specific recommendations based on the nature of road conditions that help improve road safety and driving.

## 4. RESULTS AND DISCUSSION

In this section, we disclose the outcomes and comparative evaluation of our devised intelligent transportation-driven smart driver assistance systems, benchmarked against existing solutions. To ascertain the effectiveness of our proposed system, validation is conducted employing publicly accessible datasets, namely IDMT traffic, LSA, and ROA. The implementation of our proposed MCO-EPO-RANN system is executed within the Google Colab environment using the Python programming language. The performance of our system is juxtaposed with established state-of-the-art systems, employing diverse metrics including accuracy, precision, recall, and F-measure for a comprehensive comparative analysis.

### 4.1 Dataset description

To validate the effectiveness of our proposed system, validation is conducted employing publicly accessible datasets, namely IDMT traffic, LSA, and ROA.

- **IDMT traffic dataset [30]:** It contains 15,706 2-second lengthy sound system brief snippets, which were removed from 4718 vehicle passing occasions caught with both excellent sE8 and mid-range quality MEMS amplifiers at two recording areas with speed cutoff points of 30 and 50 km/h. As the test set, recordings were used from the third location with a speed limit of 70 km/h. The IDMT traffic dataset is broken down into categories in **Table 2** by the number of samples in each class. The dataset is separated into three sets: preparing, approval, and testing. For each set, the number of samples is specified for both normal traffic and abnormal traffic conditions. In the training set, there

are 2393 samples representing normal traffic and 2893 samples for abnormal traffic. The validation set consists of 266 samples for normal traffic and 322 samples for abnormal traffic. Finally, the testing set includes 1412 samples for normal traffic and 1445 samples for abnormal traffic. The total for the entire dataset sums up to 4071 samples for normal traffic and 4660 samples for abnormal traffic, encompassing all training, validation, and testing sets. We prepared all brain networks utilizing the Adam enhancer for 250 ages with a learning pace of 10<sup>-5</sup>. Early halting with the persistence of 50 ages is utilized on the approval misfortune to screen the preparation interaction.

**Table 2:** Description of IDMT traffic dataset

Number of samples	Normal traffic	Abnormal traffic
Training	2393	2893
Validation	266	322
Testing	1412	1445
Total	4071	4660

- LSA vehicle dataset[31]:** A receiver mounted on the HD camera is utilized to catch an emergency vehicle on the streets. NCBC-ZU lab has introduced mouthpiece-coordinated HD cameras in twenty unique areas in Karachi. Nonetheless, just four areas have been chosen for information assortment. **Table 3** provides a detailed description of the LSA vehicle dataset, outlining key characteristics and attributes. The dataset consists of two distinct categories: Emergency Siren Sounds and Road Noise. There are 900 samples for each category, resulting in a total of 1800 samples in the dataset. The total duration of the audio clips is 3.15 hours, with individual clips having lengths ranging from 3 to 15 seconds. The audio clips are recorded at a sampling rate of 48 kHz, ensuring high-quality audio data for analysis. This dataset is specifically curated to capture and differentiate between emergency sirens and road noise, contributing to the comprehensive evaluation of the proposed system's performance.

**Table 3:** Description of the LSA vehicle dataset

Description	Values
Emergency Siren Sounds	900
Road noise	900
Total samples	1800
Total duration	3.15 hours
Audio clip length	3-15 seconds
Sampling rate	48 kHz

- RQA road dataset [32]:** It accumulates information from a few inactive methodologies. For information assortment, two sensor networks were utilized, every one comprising of single-board PC (SBC) Raspberry Pi and MPU-9250 modules, everyone furnished with an accelerometer, gyator, magnetometer, and temperature sensor. An outside GPS source was likewise utilized, creating area and speed information, as well as a camera for catching encompassing video. The RQA road dataset, which includes three distinct road types, is presented in detail in **Table 4**, which provides: Rough, Smooth, and Grassy. In the training set, the dataset includes 5689 samples of Rough Road, 7458 samples of Smooth Road, and 6325 samples of Grassy Road. For the validation set, there are 1568 samples of Rough Road, 2154 samples of Smooth Road, and 1898 samples of Grassy Road. The testing set consists of 2300 samples for each road type. In total, the dataset comprises 19,472 training samples, 5620 validation samples, and 6900 testing samples.

**Table 4:** Description of the RQA road dataset

Road type	Training	Validation	Testing
Rough	5689	1568	2300
Smooth	7458	2154	2300
Grassy	6325	1898	2300
Total samples	19472	5620	6900

## 4.2 Comparative analysis

### 4.2.1 Result comparison for IDMT traffic dataset

In this section, we validate the performance of proposed and existing ITS with ADAS systems using the IDMT traffic dataset. The results of our MCO-EPO-RANN system are compared with the existing state-of-art systems such as nearest neighbor[33], bayer's[34], random forest[35], support vector machine (SVM)[36], artificial neural network (ANN)[37], and Neuro-Fuzzy [38]. **Table 5** describes the comparative analysis of the IDMT traffic dataset with the training dataset. In terms of accuracy, the nearest neighbor system achieves 65.147%, followed by Bayer's at 70.383%, Random Forest at 75.619%, SVM at 80.855%, ANN at 86.091%, Neuro-Fuzzy at 91.327%, and finally, the proposed MCO-EPO-RANN system excels with an impressive 96.563%. This shows a substantial increase in accuracy with the proposed system. Precision, measuring the system's ability to correctly identify positive instances, follows a similar trend. The Nearest Neighbor system starts at 64.273%, progressing through the systems until the MCO-EPO-RANN system attains the highest precision at 95.689%. The proposed system exhibits an improvement in precision compared to the existing methods. Recall, indicating the system's capability to capture all positive instances, shows consistent improvement across systems. The Nearest Neighbor system starts at 63.819%, reaching its peak with the MCO-EPO-RANN system at 95.235%. This demonstrates the effectiveness of the proposed system in identifying abnormal traffic instances. F-measure, a harmonic mean of precision and recall, follows a similar pattern. MCO-EPO-RANN system achieves the highest F-measure at 95.461%, emphasizing balanced performance in both precision and recall.

The results for the testing phase further underscore the superior performance of the proposed MCO-EPO-RANN system compared to existing systems in the IDMT traffic dataset. In terms of accuracy, the Nearest Neighbor system starts at 82.478%, followed by Bayer's at 85.041%, Random Forest at 87.604%, SVM at 90.167%, ANN at 92.730%, Neuro-Fuzzy at 95.293%, and finally, the MCO-EPO-RANN system excels with an outstanding accuracy of 97.856%. This reflects a remarkable increase in accuracy for the proposed system. Precision, indicating the ability to correctly identify positive instances, exhibits a consistent improvement across systems.

**Table 5:** Comparative analysis of proposed and existing systems for IDMT traffic dataset

System	Values in %			
	Accuracy	Precision	Recall	F-measure
Testing				
Nearest Neighbor [33]	65.147	64.273	63.819	64.045
Bayer's [34]	70.383	69.509	69.055	69.281
Random Forest [35]	75.619	74.745	74.291	74.517
SVM [36]	80.855	79.981	79.527	79.753
ANN [37]	86.091	85.217	84.763	84.989
Neuro-Fuzzy [38]	91.327	90.453	89.999	90.225
MCO-EPO-RANN [39]	96.563	95.689	95.235	95.461
Training				
Nearest Neighbor [33]	82.478	81.176	79.645	79.767
Bayer's [34]	85.041	83.739	82.208	82.330
Random Forest [35]	87.604	86.302	84.771	84.893
SVM [36]	90.167	88.865	87.334	87.456
ANN [37]	92.730	91.428	89.897	90.019
Neuro-Fuzzy [38]	95.293	93.991	92.460	92.582
MCO-EPO-RANN [39]	98.856	96.554	95.023	95.145

The Nearest Neighbor system starts at 81.176%, progressing through the systems until the MCO-EPO-RANN system attains the highest precision at 96.554%. This signifies a substantial enhancement in precision with the proposed methodology. Similarly, recall, measuring the system's capability to capture all positive instances, demonstrates a notable improvement. The Nearest Neighbor system starts at 79.645%, reaching its peak with the MCO-EPO-RANN system at 95.023%. This highlights the effectiveness of the proposed system in identifying abnormal traffic instances during the testing phase. F-measure, reflecting the harmonic mean of precision and recall, follows a parallel trend. The proposed MCO-EPO-RANN system achieves the highest F-measure at 95.145%, underlining its balanced performance in both precision and recall during the testing phase. **Figures 5 and 6** show the proposed MCO-EPO-RANN

system outperforms existing systems in accuracy, precision, recall, and F-measure, indicating its superior ability to detect abnormalities in the IDMT traffic dataset with training and testing datasets, respectively.

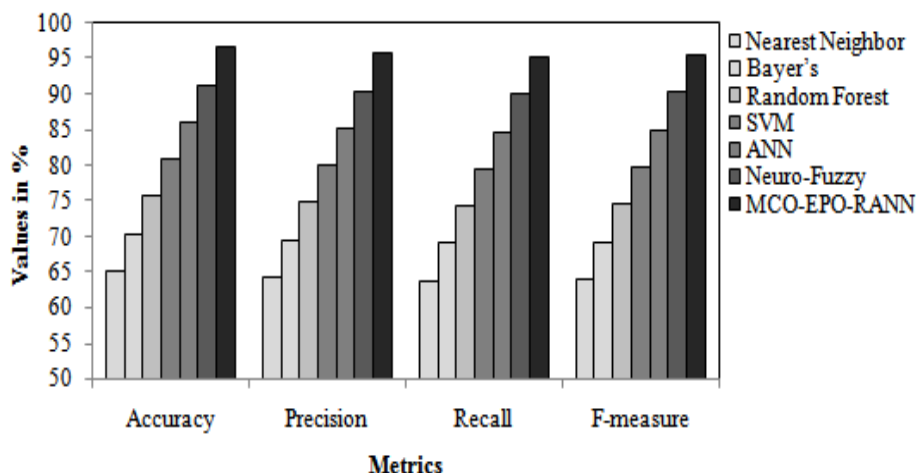


Figure 5. Results comparison of training dataset for IDMT traffic dataset

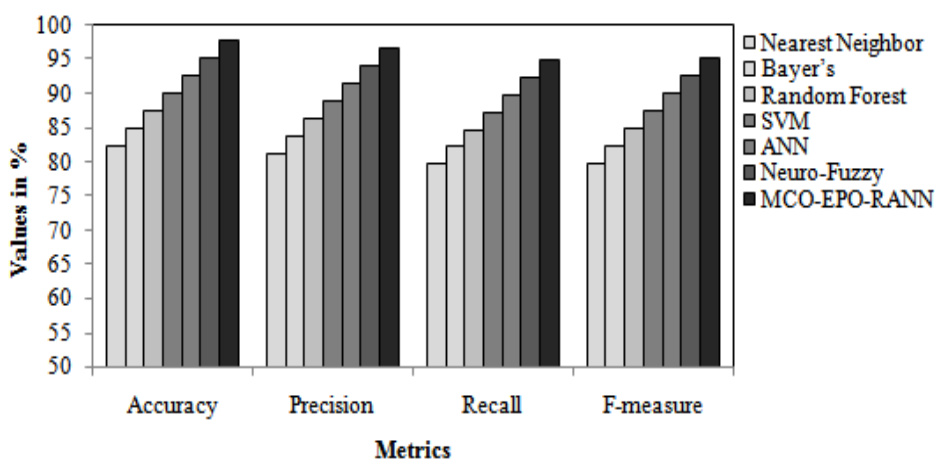


Figure 6 Results comparison of the testing dataset for the IDMT traffic dataset

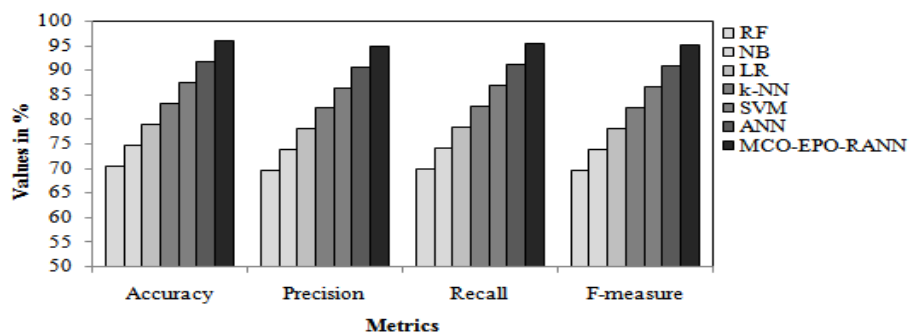
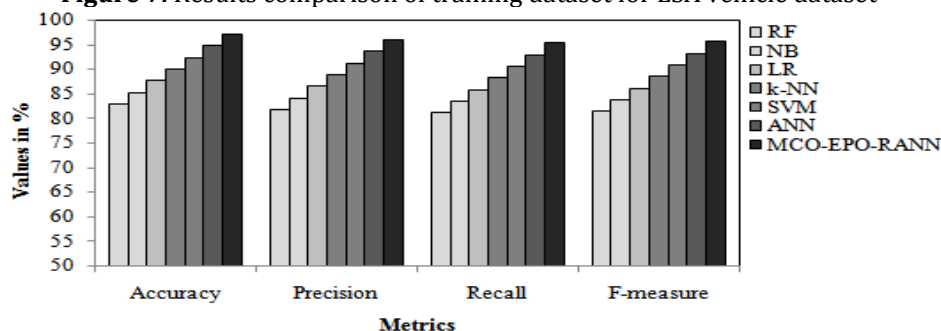
#### 4.2.2 Result comparison for LSA vehicle dataset

In this section, we validate the performance of proposed and existing ITS with ADAS systems using the LSA vehicle dataset. The results of our MCO-EPO-RANN system are compared with the existing benchmark systems such as random forest (RF) [38], Naive Bayes (NB) [39], linear regression (LR) [40], k-nearest neighbor (k-NN) [33], SVM [36], and ANN [37]. **Table 6** describes the comparative analysis of the LSA traffic dataset with the training dataset. The comparative analysis of the training phase for the LSA vehicle dataset reveals notable insights into the performance of various systems, including the proposed MCO-EPO-RANN methodology. In terms of accuracy, the RF system starts at 70.459%, followed by NB at 74.694%, LR at 78.929%, k-NN at 83.164%, SVM at 87.399%, ANN at 91.634%, and the MCO-EPO-RANN system excelling with an accuracy of 95.869%. This illustrates a substantial increase in accuracy for the proposed methodology, showcasing its effectiveness in the training phase. Precision, measuring the accuracy of positive predictions, consistently improves across systems. The RF system starts at 69.446%, progressing through the systems until the MCO-EPO-RANN system achieves the highest precision at 94.856%. This indicates a significant enhancement in precision with the proposed methodology. Similarly, recall, indicating the system's ability to identify all positive instances, exhibits a steady improvement. The RF system begins at 69.825%, reaching its zenith with the MCO-EPO-RANN system at 95.235%. This underscores the efficiency of the proposed system in capturing emergency vehicle sirens and road noises during the training phase. F-measure, representing the harmonic mean of precision and recall, mirrors the trends observed in precision and recall. The MCO-EPO-RANN system attains the highest F-measure at 95.045%, affirming its balanced performance in both precision and recall during the training phase.

**Table 6:** Comparative analysis of proposed and existing systems for the LSA vehicle dataset

System	Values in %			
	Accuracy	Precision	Recall	F-measure
	Testing			
RF [38]	70.459	69.446	69.825	69.635
NB [39]	74.694	73.681	74.060	73.870
LR [40]	78.929	77.916	78.295	78.105
k-NN [33]	83.164	82.151	82.530	82.340
SVM [36]	87.399	86.386	86.765	86.575
ANN [37]	91.634	90.621	91.000	90.810
MCO-EPO-RANN	95.869	94.856	95.235	95.045
	Training			
RF [38]	82.797	81.666	81.041	81.352
NB [39]	85.162	84.031	83.406	83.717
LR [40]	87.527	86.396	85.771	86.082
k-NN [33]	89.892	88.761	88.136	88.447
SVM [36]	92.257	91.126	90.501	90.812
ANN [37]	94.622	93.491	92.866	93.177
MCO-EPO-RANN	96.987	95.856	95.231	95.542

In the testing phase, the comparative analysis provides a comprehensive evaluation of the proposed MCO-EPO-RANN methodology against existing systems. The RF system commences with an accuracy of 82.797%, followed by NB at 85.162%, LR at 87.527%, k-NN at 89.892%, SVM at 92.257%, ANN at 94.622%, and the MCO-EPO-RANN system excels with the highest accuracy of 96.987%. Precision, reflecting the accuracy of positive predictions, consistently improves across systems. Starting at 81.666% for RF, the precision gradually rises through the systems, culminating in the MCO-EPO-RANN system achieving the highest precision at 95.856%. Recall, representing the system's ability to identify all positive instances, exhibits consistent improvement across systems. Commencing at 81.041% with RF, recall advances steadily through the systems until the MCO-EPO-RANN system achieves the highest recall at 95.231%. F-measure, combining precision and recall, follows a similar trend, with the MCO-EPO-RANN system achieving the highest F-measure at 95.542%. **Figures 7 and 8** highlight the balanced performance of the proposed methodology in accurately identifying and classifying emergency vehicle sirens and road noises during the training and testing phase.

**Figure 7.** Results comparison of training dataset for LSA vehicle dataset**Figure 8.** Results comparison of the testing dataset for the LSA vehicle dataset

### 4.2.3 Result comparison for RQA road dataset

In this section, we validate the performance of proposed and existing ITS with ADAS systems using the RQA road dataset. The results of our MCO-EPO-RANN system are compared with the existing benchmark systems such as random forest (RF) [38], Naive Bayes (NB) [39], linear regression (LR) [40], k-nearest neighbor (k-NN) [33], SVM [36] and K-means clustering (KMC) [41]. **Table 7** describes the comparative analysis for the RQA road dataset during the training phase revealing valuable insights into the performance of the proposed MCO-EPO-RANN system and existing systems. The RF system initiates the accuracy metrics at 70.446%, succeeded by NB at 74.431%, LR at 78.416%, k-NN at 82.401%, SVM at 86.386%, KMC at 90.371%, and finally, the MCO-EPO-RANN system attains the highest accuracy of 94.356%. Precision, representing the accuracy of positive predictions, consistently improves across systems. The MCO-EPO-RANN system achieves the highest precision at 94.123%, indicating the ability to precisely classify rough, smooth, and grassy road types during the training phase. Recall, which measures the system's ability to identify all positive instances, displays a consistent upward trajectory across systems. Starting at 69.742% with RF, recall gradually improves, culminating in the MCO-EPO-RANN system achieving the highest recall at 93.652%. F-measure, combining precision and recall, follows a similar trend, with the MCO-EPO-RANN system achieving the highest F-measure at 93.887%.

The testing phase comparative analysis for the RQA road dataset provides crucial insights into the performance of both the proposed MCO-EPO-RANN system and existing systems. Commencing with the RF system at 68.138% accuracy, followed by NB at 72.762%, LR at 77.385%, k-NN at 82.009%, SVM at 86.632%, KMC at 91.256%, and finally, the MCO-EPO-RANN system excels with the highest accuracy of 95.879%. Precision metrics, representing the accuracy of positive predictions, consistently improve across systems during the testing phase. MCO-EPO-RANN system achieves the highest precision at 95.016%, indicating the ability to precisely classify rough, smooth, and grassy road types. Recall, that measuring the system's ability to identify all positive instances, demonstrates a consistent upward trend across systems during testing. Commencing at 66.611% with RF, recall gradually improves, culminating in the MCO-EPO-RANN system achieving the highest recall at 94.352%. This highlights the efficacy of the proposed methodology in capturing various road types during the testing phase. F-measure, a harmonized metric of precision and recall, follows a similarly positive trend, with the MCO-EPO-RANN system achieving the highest F-measure at 94.683%. **Figures 9** and **10** indicate a well-balanced performance in accurately identifying and classifying different road types during the training and testing phases, respectively.

**Table 7:** Comparative analysis of proposed and existing systems for the RQA road dataset

System	Values in %			
	Accuracy	Precision	Recall	F-measure
	Testing			
RF [38]	70.446	70.213	69.742	69.977
NB [39]	74.431	74.198	73.727	73.962
LR [40]	78.416	78.183	77.712	77.947
k-NN [33]	82.401	82.168	81.697	81.932
SVM [36]	86.386	86.153	85.682	85.917
KMC [41]	90.371	90.138	89.667	89.902
MCO-EPO-RANN	94.356	94.123	93.652	93.887
	Training			
RF [38]	68.138	67.275	66.611	66.941
NB [39]	72.762	71.899	71.235	71.565
LR [40]	77.385	76.522	75.858	76.189
k-NN [33]	82.009	81.146	80.482	80.812
SVM [36]	86.632	85.769	85.105	85.436
KMC [41]	91.256	90.393	89.729	90.059
MCO-EPO-RANN	95.879	95.016	94.352	94.683

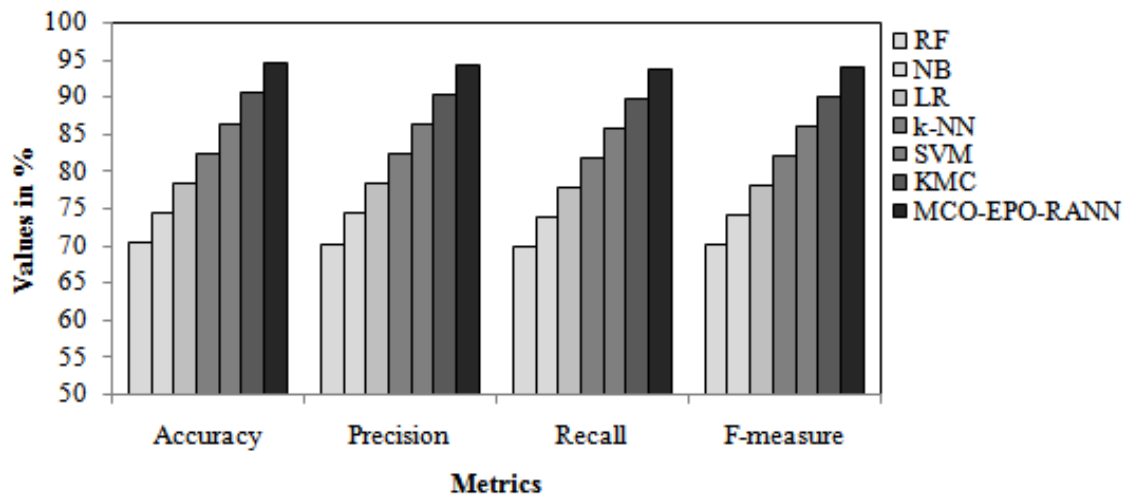


Figure 9. Results comparison of training dataset for RQA road dataset

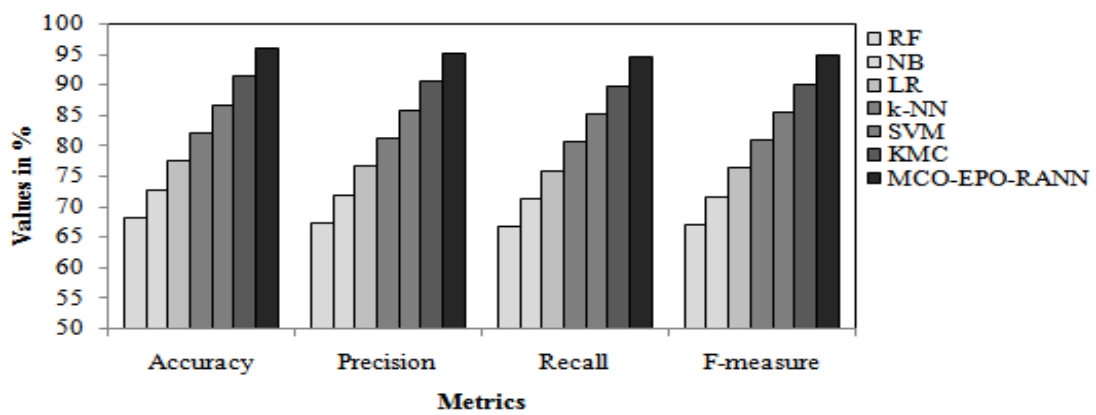


Figure 10. Results comparison of the testing dataset for the RQA road dataset

4.4 Comparative analysis of proposed and existing state-of-art techniques

Table 8 shows the comparative analysis of proposed and existing state-of-the-art techniques for ITS on smart ADAS technology. The table presents an overview of various techniques, their roles, and corresponding values in terms of accuracy, precision, recall, and F-measure. Starting with the existing methods, MIMO-NN [42], VGG-Net [43], and t-SNE [44] demonstrate accuracy values of 76.525%, 73.025%, and 69.856%, respectively, in the domain of driving assistance. SVM [36] for road accident detection achieves an accuracy of 71.245%, while XGBoost, focused on hazardous detection, records 65.235%. PGLR for vehicle-train collision detection and LPM for traffic collision detection exhibit accuracy rates of 75.234% and 89.652%, respectively. CNN-LSTM and SVM+LSTM, addressing road accident detection, show accuracies of 83.265% and 85.632%, respectively. Our MCO-EPO-RANN technique is used for smart driver assistance, outperforms these existing methods with a remarkable accuracy of 96.252%.

Table 8. Result comparison of proposed and existing state-of-art techniques for ITS for smart ADAS technology

Technique used	Role	Values in %			
		Accuracy	Precision	Recall	F-measure
MIMO-NN [42]	Driving assistance	76.525	60.344	74.185	66.552
VGG-Net [43]	Driving assistance	73.025	65.894	70.685	68.205
t-SNE [44]	Driving assistance	69.856	65.332	67.516	66.406
SVM [36]	Road accident detection	71.245	70.145	68.905	69.519
XGBoost [45]	Hazardous detection	65.235	60.198	62.895	61.517
PGLR [20]	Vehicle-train collision detection	75.234	71.247	72.894	72.061
LPM [46]	Traffic collision detection	89.652	83.698	87.312	85.467
CNN-LSTM [47]	Road accident detection	83.265	81.278	80.925	81.101

SVM+LSTM [48]	Road accident detection	85.632	72.563	83.292	77.558
MCO-EPO-RANN	Smart driver assistance	96.252	95.349	94.788	95.068

## 5. CONCLUSION

We have introduced an innovative AI-based multi-intelligent transportation system (ITS) for smart advanced driver assistance system (ADAS) technology, aimed at improving road safety and alleviating traffic congestion through the analysis of acoustic data. Our approach commences with a robust signal preprocessing phase, where the modified coati optimization (MCO) algorithm effectively eliminates unwanted artifacts from the acoustic data. Subsequently, the preprocessed signal undergoes feature extraction using the Y-Net pretrained architecture, and the extracted features are optimized using the emperor penguin optimization (EPO) algorithm to address data dimensionality issues. In the sphere of future developments, our proposed project is laying a path for further development of AI-driven driver guidance systems. In the future, blending sensor fusion methodologies will be critical in achieving a better perception of driving by fusing data from radar, LiDAR, and cameras[49]. Additionally, there is an urgent need to develop improved real-time decision-making functions that allow prompt and precise responses to changing road conditions. Behavioral analysis[50] is yet another frontier, where AI can drive insights about drivers and pedestrians to predict and prevent accidents. Integration of Vehicle-to-Everything (V2X) communication[51] will drive a networked approach to traffic management, while adaptive learning mechanisms are expected to yield continuous improvements in functionality. With aspirations shifting toward autonomous driving, our system's evolution will involve high-end algorithms for route planning, object detection, and decision-making[52]. At the same time, focus on improving user interfaces will promote trust and adoption by drivers.

## Declarations

**1. Data Availability Statement** - The data is used in the research is publicly available and can be accessed from cited articles. The code and intermediate data used in this research are available upon request by the corresponding author.

**2. Funding** Not applicable

**3. Conflict of interest** The authors declare that they have no conflict of interest.

**4. Ethical approval** The article does not contain any studies with human participants or animals performed by authors.

## REFERENCES

- [1] Bhattarai, K., Conway, D., Bhattarai, K., & Conway, D. (2021). Urban growth. *Contemporary Environmental Problems in Nepal: Geographic Perspectives*, 201-334.
- [2] Mustapha, U. F., Alhassan, A. W., Jiang, D. N., & Li, G. L. (2021). Sustainable aquaculture development: a review on the roles of cloud computing, internet of things and artificial intelligence (CIA). *Reviews in Aquaculture*, 13(4), 2076-2091.
- [3] Rahim, M. A., Rahman, M. A., Rahman, M. M., Asyhari, A. T., Bhuiyan, M. Z. A., & Ramasamy, D. (2021). Evolution of IoT-enabled connectivity and applications in automotive industry: A review. *Vehicular Communications*, 27, 100285.
- [4] Szeliski, R. (2022). *Computer vision: algorithms and applications*. Springer Nature.
- [5] LeCun, Y., Bengio, Y., & Hinton, G. (2015). Deep learning. *nature*, 521(7553), 436-444.
- [6] Nidamanuri, J., Nibhanupudi, C., Assfalg, R., & Venkataraman, H. (2021). A progressive review: Emerging technologies for ADAS driven solutions. *IEEE Transactions on Intelligent Vehicles*, 7(2), 326-341.
- [7] Ismail, W. N., PP, F. R., & Ali, M. A. (2023). A meta-heuristic multi-objective optimization method for alzheimer's disease detection based on multi-modal data. *Mathematics*, 11(4), 957.
- [8] SS, V. C., & HS, A. (2022). Nature inspired meta heuristic algorithms for optimization problems. *Computing*, 104(2), 251-269.
- [9] Tiwari, A. (2023). A hybrid feature selection method using an improved binary butterfly optimization algorithm and adaptive  $\beta$ -hill climbing. *IEEE Access*.
- [10] Tiwari, A., & Chaturvedi, A. (2023). Automatic EEG channel selection for multiclass brain-computer interface classification using multiobjective improved firefly algorithm. *Multimedia Tools and Applications*, 82(4), 5405-5433.
- [11] Tiwari, A., & Chaturvedi, A. (2022). A hybrid feature selection approach based on information theory and dynamic butterfly optimization algorithm for data classification. *Expert Systems with Applications*, 196, 116621.



- [12] Gad, A. G. (2022). Particle swarm optimization algorithm and its applications: a systematic review. *Archives of computational methods in engineering*, 29(5), 2531-2561.
- [13] Bahrami, B., Khayyambashi, M. R., & Mirjalili, S. (2023). Edge server placement problem in multi-access edge computing environment: models, techniques, and applications. *Cluster Computing*, 26(5), 3237-3262.
- [14] Dehghani, M., Montazeri, Z., Trojovská, E., & Trojovský, P. (2023). Coati Optimization Algorithm: A new bio-inspired metaheuristic algorithm for solving optimization problems. *Knowledge-Based Systems*, 259, 110011.
- [15] Dhiman, G., & Kumar, V. (2018). Emperor penguin optimizer: A bio-inspired algorithm for engineering problems. *Knowledge-Based Systems*, 159, 20-50.
- [16] Kim, J., & Kum, D. (2017). Collision risk assessment algorithm via lane-based probabilistic motion prediction of surrounding vehicles. *IEEE Transactions on Intelligent Transportation Systems*, 19(9), 2965-2976.
- [17] Chen, Y., Ardila-Gomez, A., & Frame, G. (2017). Achieving energy savings by intelligent transportation systems investments in the context of smart cities. *Transportation Research Part D: Transport and Environment*, 54, 381-396.
- [18] Nozaki, D., Okamoto, K., Mochida, T., Qi, X., Wen, Z., Tokuda, K., ... & Tamesue, K. (2018, November). AI management system to prevent accidents in construction zones using 4K cameras based on 5G network. In *2018 21st International Symposium on Wireless Personal Multimedia Communications (WPMC)* (pp. 462-466). IEEE.
- [19] Zhang, M., Zhang, Y., Zhang, L., Liu, C., & Khurshid, S. (2018, September). Deeproad: Gan-based metamorphic testing and input validation framework for autonomous driving systems. In *Proceedings of the 33rd ACM/IEEE International Conference on Automated Software Engineering* (pp. 132-142).
- [20] Singhal, V., Jain, S. S., Anand, D., Singh, A., Verma, S., Rodrigues, J. J., ... & Iwendi, C. (2020). Artificial intelligence enabled road vehicle-train collision risk assessment framework for unmanned railway level crossings. *IEEE Access*, 8, 113790-113806.
- [21] Saleem, M., Abbas, S., Ghazal, T. M., Khan, M. A., Sahawneh, N., & Ahmad, M. (2022). Smart cities: Fusion-based intelligent traffic congestion control system for vehicular networks using machine learning techniques. *Egyptian Informatics Journal*, 23(3), 417-426.
- [22] Wen, X., Xie, Y., Jiang, L., Pu, Z., & Ge, T. (2021). Applications of machine learning methods in traffic crash severity modelling: current status and future directions. *Transport reviews*, 41(6), 855-879.
- [23] Das, S., & Mishra, S. K. (2022). A machine learning approach for collision avoidance and path planning of mobile robot under dense and cluttered environments. *Computers and Electrical Engineering*, 103, 108376.
- [24] Chang, Y., & Edara, P. (2017, October). Predicting hazardous events in work zones using naturalistic driving data. In *2017 IEEE 20th International Conference on Intelligent Transportation Systems (ITSC)* (pp. 1-6). IEEE.
- [25] Chen, C., Zhang, G., Qian, Z., Tarefder, R. A., & Tian, Z. (2016). Investigating driver injury severity patterns in rollover crashes using support vector machine models. *Accident Analysis & Prevention*, 90, 128-139.
- [26] Shen, X., & Wei, S. (2020). Application of XGBoost for hazardous material road transport accident severity analysis. *IEEE Access*, 8, 206806-206819.
- [27] Tang, S., Zou, Y., Zhang, H., Zhang, Y., & Kong, X. (2024). Application of CNN-LSTM Model for Vehicle Acceleration Prediction Using Car-following Behavior Data. *Journal of Advanced Transportation*, 2024.
- [28] Feng, Y., & Yan, X. (2022). Support vector machine based lane-changing behavior recognition and lateral trajectory prediction. *Computational Intelligence and Neuroscience*, 2022.
- [29] Tonni, S. I., Aka, T. A., Antik, M. M., Taher, K. A., Mahmud, M., & Kaiser, M. S. (2021, February). Artificial intelligence based driver vigilance system for accident prevention. In *2021 International Conference on Information and Communication Technology for Sustainable Development (ICT4SD)* (pp. 412-416). IEEE.
- [30] Abeßer, J., Gourishetti, S., Kátai, A., Clauß, T., Sharma, P. and Liebetrau, J., 2021, August. IDMT-traffic: an open benchmark dataset for acoustic traffic monitoring research. In *2021 29th European Signal Processing Conference (EUSIPCO)* (pp. 551-555). IEEE.
- [31] Asif, M., Usaid, M., Rashid, M., Rajab, T., Hussain, S. and Wasi, S., 2022. Large-scale audio dataset for emergency vehicle sirens and road noises. *Scientific data*, 9(1), p.599.

- [32] Menegazzo, J. and von Wangenheim, A., 2021. Road surface type classification based on inertial sensors and machine learning: A comparison between classical and deep machine learning approaches for multi-contextual real-world scenarios. *Computing*, 103(10), pp.2143-2170.
- [33] V. P. Warghade and M. S. Deshpande, "Road Traffic Condition Estimation Based on Road Acoustics", *Proceedings of the International Conference on Computing Communication Control and Automation (ICCUBEA)*, pp. 1-5, 2017.
- [34] V. Tyagi, S. Kalyanaraman and R. Krishnapuram, "Vehicular Traffic Density State Estimation Based on Cumulative Road Acoustics", *IEEE Transactions on Intelligent Transportation Systems*, vol. 13, no. 3, pp. 1156-1166, 2012.
- [35] R. C. Gatto and C. H. Q. Forster, "Audio-Based Machine Learning Model for Traffic Congestion Detection", *IEEE Transactions on Intelligent Transportation Systems*, pp. 1-8, 2020.
- [36] S. Djukanovic, J. Matas and T. Virtanen, "Robust Audio-Based Vehicle Counting in Low-to-Moderate Traffic Flow", *Proceedings of the IEEE Intelligent Vehicles Symposium (IV)*, pp. 1608-1614, 2020.
- [37] Shiping Chen, Ziping Sun and B. Bridge, "Traffic Monitoring Using Digital Sound Field Mapping", *IEEE Transactions on Vehicular Technology*, vol. 50, no. 6, pp. 1582-1589, 2001.
- [38] Rigatti, S. J. (2017). Random forest. *Journal of Insurance Medicine*, 47(1), 31-39.
- [39] Webb, G. I., Keogh, E., & Miikkulainen, R. (2010). Naïve Bayes. *Encyclopedia of machine learning*, 15(1), 713-714.
- [40] Su, X., Yan, X., & Tsai, C. L. (2012). Linear regression. *Wiley Interdisciplinary Reviews: Computational Statistics*, 4(3), 275-294.
- [41] Burkhart, J. (2009). K-means clustering. Virginia Tech, Advanced Research Computing, Interdisciplinary Center for Applied Mathematics.
- [42] Ferianc, M., & Rodrigues, M. (2023). MIMMO: Multi-Input Massive Multi-Output Neural Network. In *Proceedings of the IEEE/CVF Conference on Computer Vision and Pattern Recognition* (pp. 4564-4569).
- [43] Simonyan, K., & Zisserman, A. (2014). Very deep convolutional networks for large-scale image recognition. *arXiv preprint arXiv:1409.1556*.
- [44] Van Der Maaten, L. (2014). Accelerating t-SNE using tree-based algorithms. *The journal of machine learning research*, 15(1), 3221-3245.
- [45] Chen, T., & Guestrin, C. (2016, August). Xgboost: A scalable tree boosting system. In *Proceedings of the 22nd acmsigkdd international conference on knowledge discovery and data mining* (pp. 785-794).
- [46] Ijjina, E. P., Chand, D., Gupta, S., & Goutham, K. (2019, July). Computer vision-based accident detection in traffic surveillance. In *2019 10th International conference on computing, communication and networking technologies (ICCCNT)* (pp. 1-6). IEEE.
- [47] Cura, A., Küçük, H., Ergen, E., & Öksüzöğlü, İ. B. (2020). Driver profiling using long short term memory (LSTM) and convolutional neural network (CNN) methods. *IEEE Transactions on Intelligent Transportation Systems*, 22(10), 6572-6582.
- [48] Ali, F., Ali, A., Imran, M., Naqvi, R. A., Siddiqi, M. H., & Kwak, K. S. (2021). Traffic accident detection and condition analysis based on social networking data. *Accident Analysis & Prevention*, 151, 105973.
- [49] Bharathi, D., Karthi, R., & Geetha, P. (2023, October). Blending of Landsat and Sentinel images using Multi-sensor fusion. In *Journal of Physics: Conference Series* (Vol. 2571, No. 1, p. 012008). IOP Publishing.
- [50] Millenson, J. R., & Leslie, J. C. (1967). *Principles of behavioral analysis* (pp. 43-44). New York: Macmillan.
- [51] Noor-A-Rahim, M., Liu, Z., Lee, H., Khyam, M. O., He, J., Pesch, D., ... & Poor, H. V. (2022). 6G for vehicle-to-everything (V2X) communications: Enabling technologies, challenges, and opportunities. *Proceedings of the IEEE*, 110(6), 712-734.
- [52] Pera, A. (2022). The moral decision-making capacity of autonomous mobility technologies: Route planning algorithms, simulation modeling tools, and intelligent traffic monitoring systems. *Contemporary Readings in Law and Social Justice*, 14(2), 136-153.